Nuclear Instruments and Methods in Physics Research A309 (1991) 77–100
North-Holland

NUCLEAR
INSTRUMENTS
& METHODS
IN PHYSICS
RESEARCH
Section A

Design and construction of the ZEUS barrel calorimeter

M. Derrick, D. Gacek, N. Hill, B. Musgrave, R. Noland, E. Petereit,
J. Repond, R. Stanek and K. Sugano [1]
Argonne National Laboratory, Argonne, IL 60439, USA

Received 6 June 1991

We present the mechanical design and construction techniques used in building the barrel calorimeter for the ZEUS detector. The latter is currently under construction for use at the HERA electron–proton colliding beam facility. The calorimeter consists of 32 wedge shaped modules with approximate dimensions of $3\times0.5\times1.7$ m^3. The modules use alternate layers of depleted uranium and scintillator with one radiation length sampling. The light is collected via wavelength shifter plates placed on the sloping sides of the modules and read out by photomultiplier tubes located at the outer radius. The unit cell dimensions result in a ratio $e/h=1$ which yields an optimal energy resolution for hadronic jets. The placing of the structural components and the arrangement of the cracks between modules were chosen to maximize the uniformity of the response. Details of the construction and assembly effort needed to realize the total calorimeter are given. We finally describe the procedures used for transporting the completed modules to DESY and to install them on ZEUS.

1. Introduction

The HERA electron–proton colliding beam facility under construction at the DESY laboratory in Hamburg, Germany, will start operation in the fall of 1991. The design luminosity, $\mathscr{L}=16\times10^{30}$ cm^{-2} s^{-1}, is expected to be achieved after one or two years of running. The facility will extend deep inelastic scattering studies into the momentum transfer region above 10^4 GeV^2 and give rise to events with maximum laboratory energies of the current jet and of the electron from 30 to 800 GeV, depending on the scattering angle. Two general purpose detectors are currently under construction to study electron–proton collisions at HERA: H1 and ZEUS. The ZEUS detector [1] has been built by an international collaboration involving 46 institutions from 10 different countries. The technical proposal was submitted in March 1986 and approved in November of the same year.

Fig. 1 shows an overview of the ZEUS detector. The asymmetry in the beam energies leads to an asymmetric design with additional tracking and a deeper calorimeter in the direction of the proton beam. The main features of the detector include charged particle tracking over almost the full solid angle, hermetic, high-resolution calorimetry, excellent lepton identification, leading proton and forward electron and photon detection. To achieve these goals the following major components are provided: a vertex chamber, a central tracking system with capability of measuring $\mathrm{d}E/\mathrm{d}x$, a forward tracking system including transition radiation detectors, a superconducting solenoid, a high resolution calorimeter, an iron backing calorimeter and a muon detection system that utilizes the toroidally magnetized return yoke in the central region and additional toroids in the forward direction.

The design emphasizes precision energy measurements for hadronic jets, since accurate measurement of such jets is crucial to the determination of the proton structure functions extracted from both charged and neutral current events. Over almost the entire kinematical range the precision of measurement of the structure functions is dictated by the resolution of the energy measurement of the hadronic jet.

In this article we describe in detail the design and construction of the central part of the high resolution calorimeter, called the barrel calorimeter (BCAL). We also discuss transportation of the modules between the construction sites and DESY and the installation on the ZEUS detector.

2. The high resolution calorimeter

The calorimeter for the ZEUS detector was designed to give the best possible resolution in the measurement of hadronic jets, to present a homogeneous

[1] Now at Institute for Particle Physics, University of California, Santa Cruz, CA 95064, USA.

response over most of the solid angle and to have a good resolution for electromagnetic showers. The calorimeter consists of two parts: a high resolution inner section and a lower resolution backing calorimeter. The latter is provided by the iron return yoke for the central magnetic field segmented into 73 mm thick plates and instrumented with proportional tubes, see fig. 1. The purpose of the backing calorimeter is primarily to tag jets with substantial leakage out of the high resolution calorimeter. The energy resolution is $\sigma_{E_{had}} \sim 100\%/\sqrt{E[\mathrm{GeV}]}$ and the 10 layers of iron in the barrel region correspond to a thickness of 4.3λ.

In order to achieve the best energy resolution in a calorimeter, the response to the electromagnetic and the hadronic parts of jets must be equal, expressed as $e/h = 1$. Typically, calorimeters of existing collider detectors are undercompensating, i.e. the electromagnetic response is substantially larger than the hadronic response, e.g. $e/h \gtrsim 1.5$. Compensation is achieved both by enhancement of the hadronic response and by suppression of the electromagnetic response [2]. The hadronic response can be enhanced by efficient detection of the neutron component of hadronic showers as well as detection of γ-rays coming from nuclear deexcitation, while the electromagnetic component can be suppressed by choosing a high-Z material as radiator.

At the time of the design of the ZEUS detector, a sampling calorimeter using depleted uranium (DU) as absorber and plastic scintillator as active material was the only technology known to both achieve $e/h = 1$, within a few percent and to have an acceptable resolution for electromagnetic showers.

The unit cell is about 8 mm and contains 3.3 mm DU, which corresponds to one radiation length ($1X_0$), and 2.6 mm of scintillator. An air gap is provided to ensure that the scintillator is not subject to pressure caused by irregularities in the manufacture of the DU plates. This particular choice of parameters yields a jet energy resolution $\sigma_{E_{had}} = 35\%/\sqrt{E[\mathrm{GeV}]}$ and a resolution for electromagnetic showers $\sigma_{E_{em}} = 18\%/\sqrt{E[\mathrm{GeV}]}$. These resolutions were demonstrated in test beam measurements at CERN [3] and corrobo-

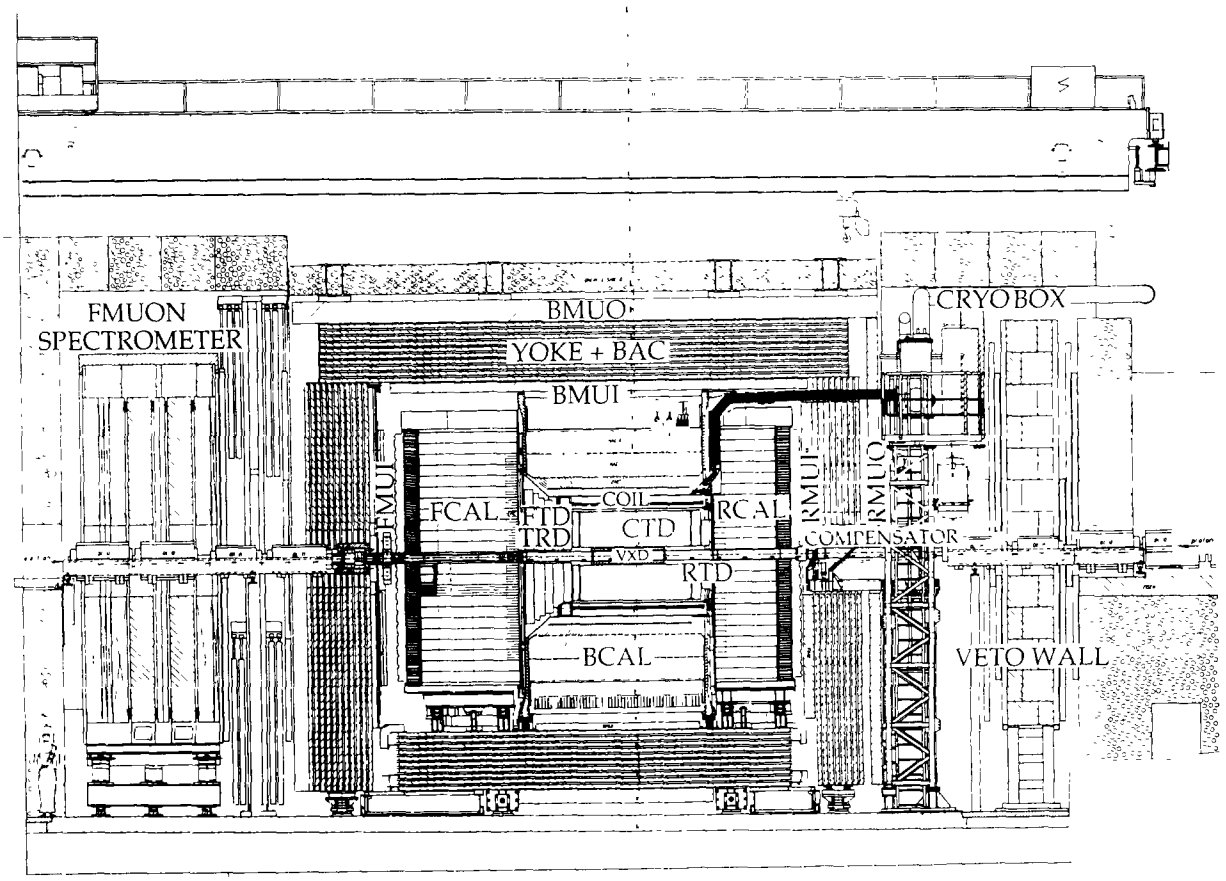

Fig. 1. Cross section in the plane parallel to the beam axis through the ZEUS detector showing its major components.

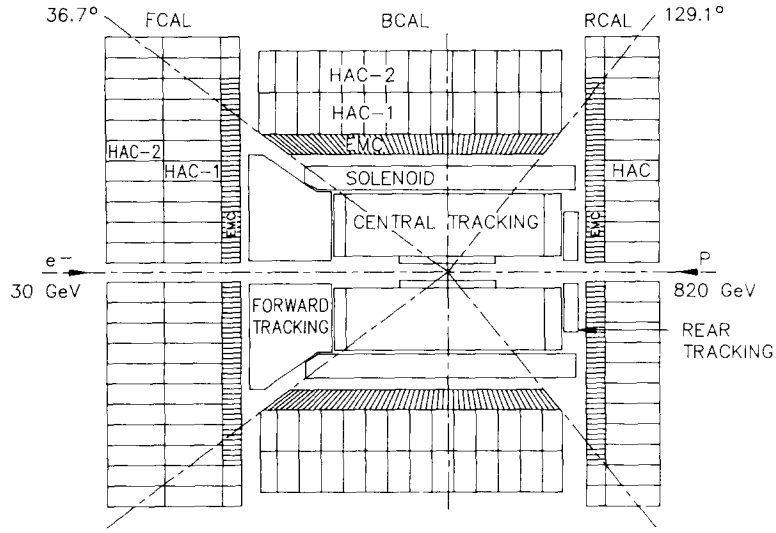

Fig. 2. Schematic of the high resolution calorimeter.

rated by Monte Carlo calculations based on the HERMES [4] and EGS4 [5] shower simulation codes. The cell structure is common to the entire high resolution calorimeter, thus ensuring a homogeneous response over a large solid angle and for the entire depth of the calorimeter.

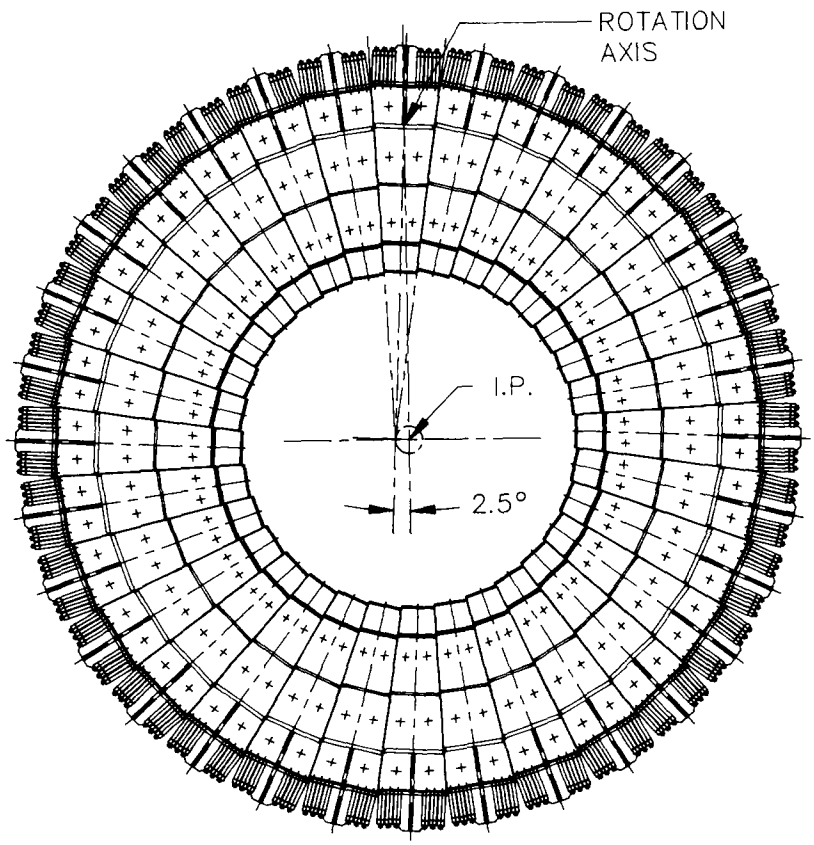

Fig. 3. Cross section through the barrel calorimeter. The electron beam direction is into the figure.

The light produced in the scintillator is read out by the standard technique of wavelength shifting and guiding to the back of the calorimeter using wavelength shifter plates. The latter are located on the two sloping sides of a module.

Fig. 2 shows a schematic of the high resolution calorimeter. It is divided into three parts:
- the forward calorimeter (FCAL) covering polar angles from $\theta = 2.2°$ to $39.9°$;
- the barrel calorimeter (BCAL) covering polar angles from $\theta = 36.7°$ to $129.1°$;
- the rear calorimeter (RCAL) covering polar angles from $\theta = 128.1°$ to $176.5°$.

The asymmetry along the beam axis reflects the kinematics of the electron–proton collisions at HERA. The depth is chosen to contain at least 95% of the energy for 90% of the hadronic jets with the highest energy kinematically allowed. This energy varies from 800 GeV in the forward direction to 30 GeV in the backward direction relative to the proton beam. In the BCAL the maximum jet energies vary from 200 GeV in the forward direction to 40 GeV at the backward angles. These depths correspond to 7 interaction lengths, λ, for the FCAL and 5λ (4λ) for the BCAL (RCAL) at normal incidence.

3. Design of the barrel calorimeter

3.1. General description

The BCAL covers the region between $\theta = 36.7°$ and $129.1°$ in polar angle and $360°$ in azimuth. It consists of 32 wedge shaped modules each spanning $11.25°$ in azimuth, as shown in fig. 3. The modules extend from an inner radius $R_1 = 1232$ mm to an outer radius $R_0 = 2912$ mm from the beam axis. Each module is rotated by $2.5°$ clockwise in the azimuthal plane around an axis parallel to the beam axis and located at a radius of 2309 mm. This rotation ensures that the wavelength shifter plates do not point to the beam axis, thus preventing photons from escaping undetected in the gap between modules and so compromising the measurements of jet energies and missing transverse energy.

Each module weighs approximatively 10 tons for a total weight of 320 tons for the barrel. In the overall BCAL structure the modules are attached at their front and rear to two large aluminum discs, referred to as the spokeswheels, whose thickness varies between 50 and 130 mm, depending on the radius from the beam axis, as seen in fig. 4. These discs, together with

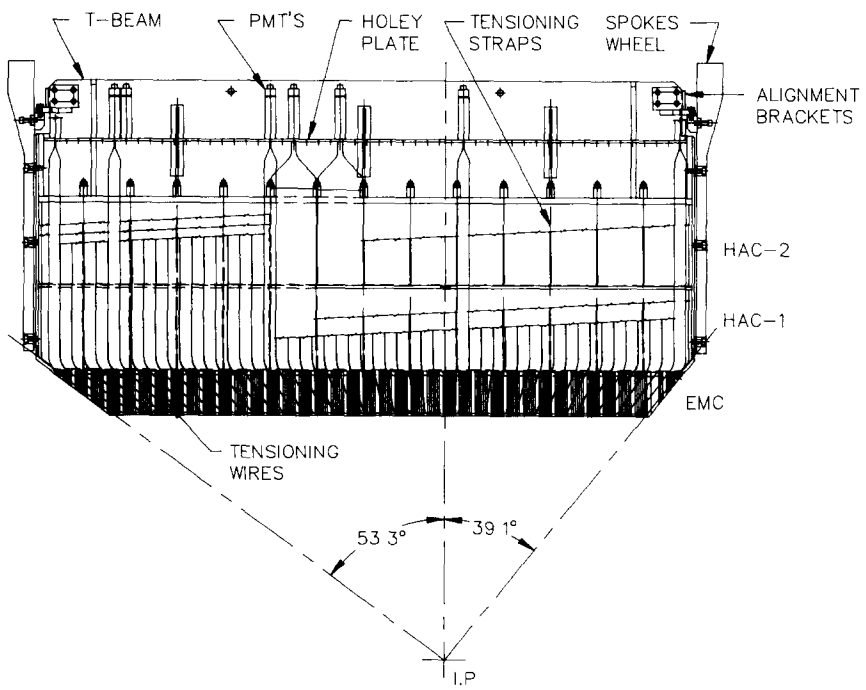

Fig. 4. Side view of a BCAL module mounted in the spokeswheels.

the modules, form a rigid structure that also supports the superconducting coil and the central tracker. The system is designed such that no other module-to-module supports are needed.

3.2. Description of a BCAL module

The modules are segmented in depth into three sections which are read out independently: one electromagnetic (EMC) and two hadronic calorimeter sections (HAC_I and HAC_{II}), see figs. 4 and 5.

The EMC section consists of 53 towers, projective in polar angle, with front face dimensions of 49×233 mm^2. Each section contains 21 DU plates, corresponding to $21 X_0$, and 22 layers of scintillator. The composition of the EMC is given in table 1. A thin walled aluminum box is inserted between the 4th layer of scintillator and the 4th DU plate of the EMC. This box is provided for housing a future fine grained detector at the maximum of the electromagnetic showers. This upgrade will significantly improve the hadron–electron separation and the angular resolution of photon induced electromagnetic showers.

The 14 HAC towers are nonprojective and, with the exception of the forward and rear ones, the scintillator plates of the first layer measure 244×271 mm^2. The composition of a HAC tower is also given in table 1.

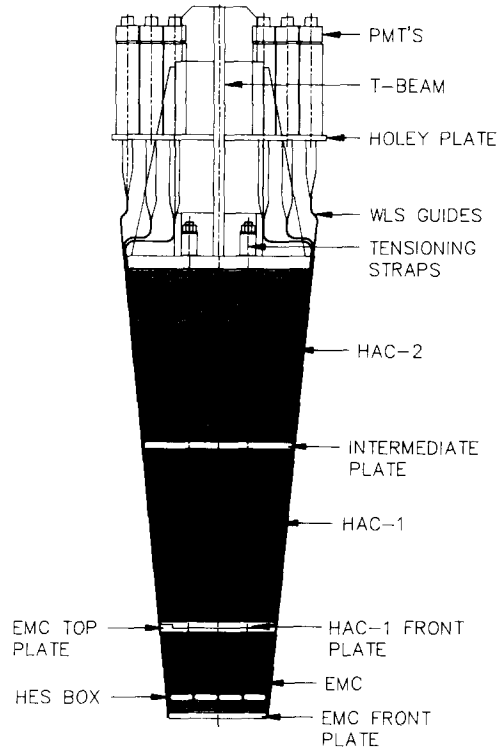

Fig. 5. Cross section through a BCAL module showing the structural elements

Table 1
Composition of the EMC and HAC sections (normal incidence)

Section	Item	Material	Number	Thickness [mm]	X_0	λ
EMC	cover	steel	1	0.2	0.01	0.001
	front plate	Al	1	12.7	0.14	0.032
	scintillator	polystyrene	22	$22 \times 2.6 = 57.2$	0.14	0.072
	DU plate	U	21	$21 \times 3.3 = 69.3$	21.0	0.660
	cladding	steel	42	$42 \times 0.2 = 8.4$	0.48	0.050
	HES box	Al	2	$2 \times 1.0 = 2.0$	0.02	0.005
	shim	steel	1	0.2	0.01	0.001
	rear plate	Al	1	10.0	0.11	0.025
	Total			213.5	21.9	0.846
HAC_I	front plate	steel	1	14.5	0.82	0.087
	scintillator	polystyrene	50	$50 \times 2.6 = 130.0$	0.31	0.164
	DU plate	U	49	$49 \times 3.3 = 161.7$	49.0	1.540
	cladding	steel	98	$98 \times 0.4 = 39.2$	2.23	0.234
	shim	Al	1	1.58	0.02	0.004
	Total			421.9	52.4	2.029
HAC_{II}	interm. plate	steel	1	17.0	0.97	0.101
	scintillator	polystyrene	50	$50 \times 2.6 = 130.0$	0.31	0.164
	DU plate	U	49	$49 \times 3.3 = 161.7$	49.0	1.540
	cladding	steel	98	$98 \times 0.4 = 39.2$	2.23	0.234
	shim	Al	1	1.58	0.02	0.004
	Total			424.4	52.5	2.043
T-beam		steel	1	30.0	1 71	0.179
Total				1089.8	128.5	5.097

Starting from the $\theta = 90°$ line four EMC towers are covered by one HAC tower. However, the front (rear) tower is narrower in width covering only 2 (3) EMC towers. Each hadronic section consists of 49 plates of DU and 50 layers of scintillator. The steel plate separating HAC_I from HAC_{II} is 17 mm thick ($1X_0$) and the composite aluminum and steel plate separating the EMC from HAC_I is also nominally $1X_0$ in thickness. The total depth of the BCAL corresponds to 5 interaction lengths for normal incidence.

3.3. Mechanical support structures for the HAC

The support structure was designed to minimize any adverse effects on the energy resolution, the homogeneity and the hermeticity of the calorimeter. Most of the structure is therefore located at the outer radius of the module.

The structural integrity of a module is provided by a frame consisting of a backbeam (T-beam), to which is bolted and pinned a front and a rear end plate. This structure is completed by an intermediate plate at the HAC_I–HAC_{II} boundary and a plate at the front of HAC_I, as seen in the photograph of fig. 6. Apart from a short aluminum extension of each end plate, all components are made of iron or steel. The end plates are carefully aligned and pinned to the T-beam and all components are held together with bolts. Three gussets are used on each side of the T-beam web to provide additional strength, when the module is in the horizontal orientation. For ease of aligning the DU plates and to increase support, a key, located on the center line, is inset into each of the end plates and their extensions.

To avoid pressure on the scintillator tiles, the DU plates are held apart by stainless steel spacers located between the scintillator tiles, as shown in fig. 7a. The spacers are chosen from three different sizes in height (3.96, 4.09 and 4.22 mm) to allow for variation in thickness of the DU plates, both from plate to plate and within a given plate. The thickness of all DU plates was measured at the position of every spacer and the appropriate spacer was chosen to maintain the required stack height. The nominal size of the unit cell for the HAC section is 8.2 mm.

A module is compressed by 13 pairs of steel straps inserted at the HAC tower boundaries between both the scintillator tiles and the columns of spacers. The cross section of the straps is 3.18×25.40 mm^2. Tension in the straps compresses a module between its front steel plate and its rear T-beam structure, see figs. 4

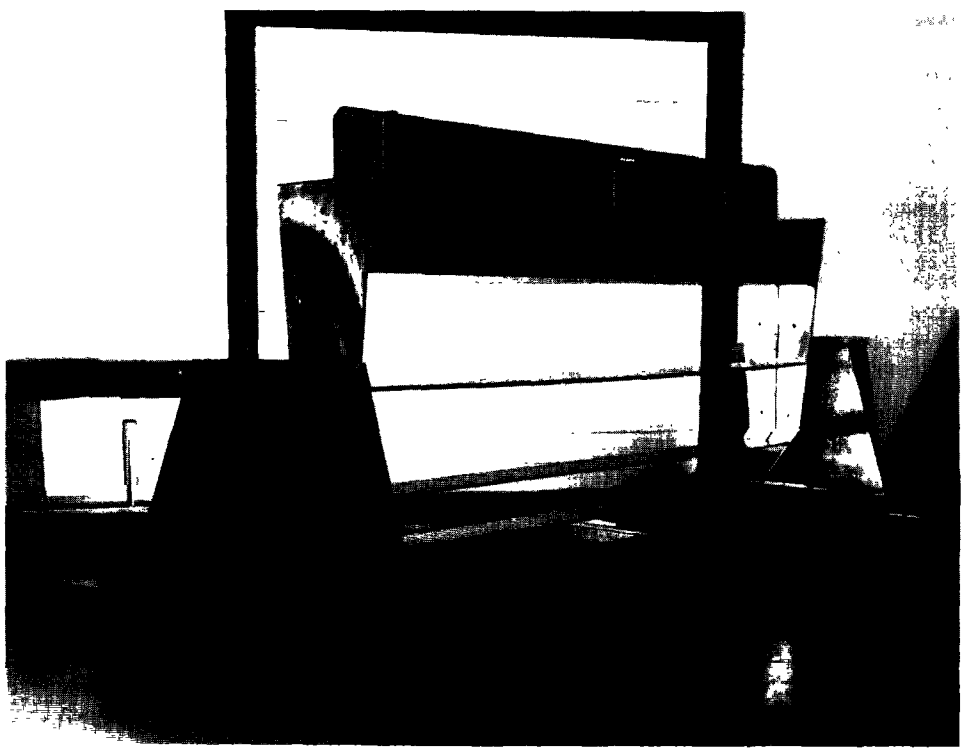

Fig. 6. Structural frame of a BCAL module showing the T-beam, the end plates, the front plate and the intermediate plate of the HAC. The EMC box is attached at the bottom.

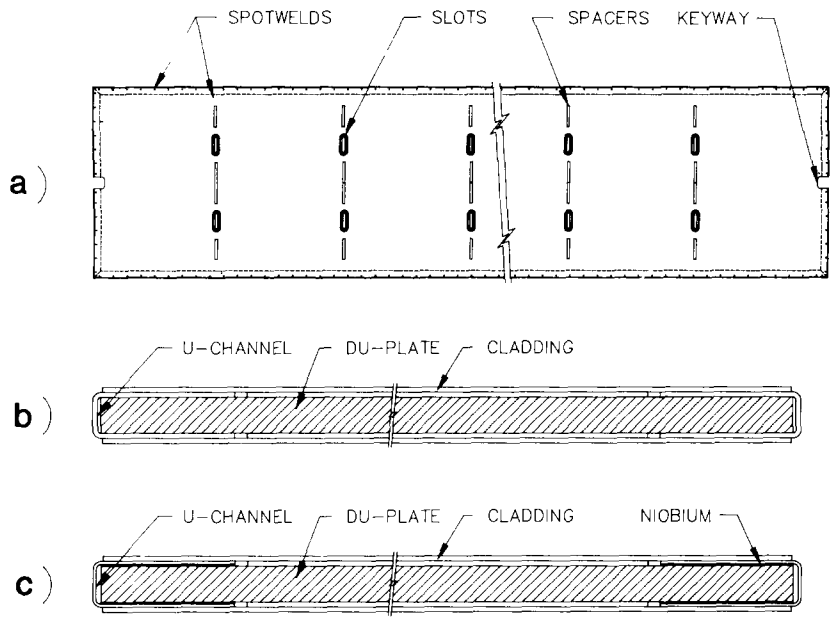

Fig. 7. Schematic of a clad DU plate: (a) top view of an HAC plate showing the location of the spacers, slots and keyways; (b) cross section through a clad HAC plate; (c) cross section through a clad EMC plate.

and 5. The tension per strap was set at approximately 3 tons giving a total compressive force on the module of more than 70 tons. The friction coefficient of 0.2 between the spacers and the stainless steel cladding of the DU plates, together with this compression, is designed to prevent any slippage of the DU plates under azimuthal rotation of the module. This support is in addition to that provided by the end plate keys.

3.4. Mechanical support structures for the EMC

In the EMC section the DU plates are held apart by aluminum I-beam spacers selected from three different sizes in height (4.17, 4.29 and 4.42 mm) according to the thickness measurements of the DU plates. The nominal size of the unit cell for the EMC section is 8.0 mm. The spacers are located between adjacent scintillator tiles, as shown in fig. 8 and span the whole width of the module. The gap between scintillator pieces is typically 1.4 mm, where 1.0 mm is taken by the web of the I-beam spacers. This results in a dip of up to 20% in the response to electromagnetic showers across the boundary [6].

The EMC stack is held together by 265 wires, each of 0.74 mm diameter, spaced 10 mm apart along the length of the module. The wires are made of an alloy of cobalt, chromium, nickel and molybdenum with a breaking tension of ~ 64 kg.

The wires, fixed at one end by a simple loop around a stainless steel rod located on either edge of the EMC top plate, are wrapped around the stack and tensioned at the other end via a tuning pin inserted into the opposite edge of the EMC top plate. The details are shown in figs. 8 and 9. The wire tensions T, on the two sides of the stack are typically 30 and 20 kg per wire, respectively. The fixed end alternates between sides so that the mean tension is the same on each side of the section. The tensions were adjusted by acoustically matching the pitch of a tensioned wire to the sound generated by a sine wave generator:

$$T[\mathrm{N}] = 4\nu^2 ml,$$

where ν is the frequency of the sine wave in Hz^{-1}, $m = 7.64 \times 10^{-4}$ kg is the mass and $l = (0.216 \pm 0.002)$ m, the length of the wire over which it can freely oscillate. The total compression of the EMC stack is approximately 13 tons.

The friction resulting from the compression of the EMC by the wires prevents both slippage and any significant deflection of the module under rotation in azimuth. The box housing the EMC consists of a front plate, two end frames and a top plate, all made of aluminum. It provides by itself only an insignificant mechanical rigidity. The top plate is not directly connected to the two end frames or to the front plate. The EMC box serves primarily as a support structure for mounting and tensioning of the wires.

The nominal diameter of the tuning pins is 5.0 mm. All pins were measured and sorted according to their diameter which varied between 4.6 and 5.4 mm. As the size of the holes in the EMC top plate also varied, pins were selected to match the holes. The inserted pins

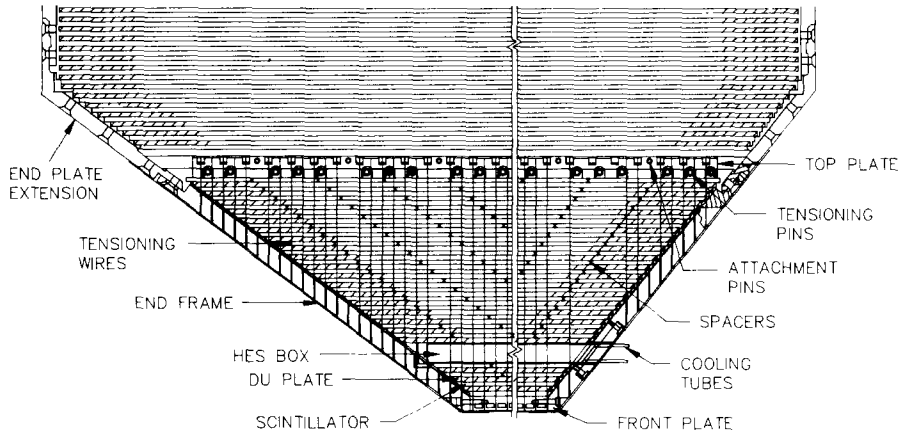

Fig. 8. Side view of the EMC section showing the forward and rear end details.

typically resisted rotation for torques as high as 7 N m which is to be compared with the maximum torque exerted by the wire, $T_{max} = 1.6$ N m. For the few holes found to be excessively oversized, the pins had to be shimmed before insertion to ensure a tight fit.

3.5. Mating the HAC and EMC

The EMC and HAC sections of a module are physically separate units and were stacked individually in separate rooms using different teams. The completed sections were mated by lowering the HAC on top of the EMC using the hydraulic system of the HAC stacking fixture. The pressure gauge of this hydraulic system was used to estimate the load of the HAC on the EMC. In order to prevent damage to the aluminum spacers of the EMC at local pressure points the load was restricted to be not more than 3 tons.

After checking the uniformity of the mating at the contact surfaces the two sections were attached by

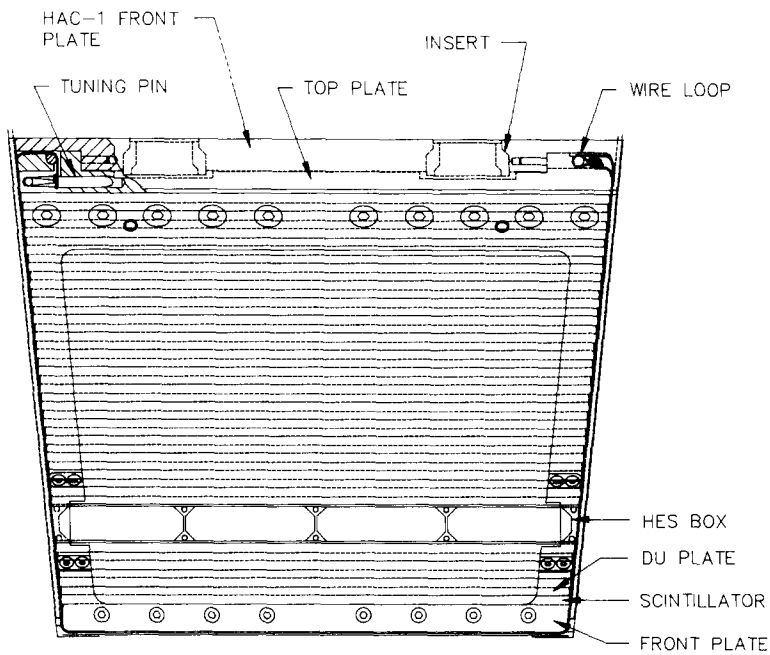

Fig. 9. Rear endview of the EMC section.

inserting 42 stainless steel shear pins connecting the EMC top plate with the HAC front plate, see figs. 8 and 10. The holes in the HAC front plate were drilled using the corresponding holes in the EMC top plate as a template, thus ensuring an optimal alignment. The 3 mm diameter connecting pins were threaded into the EMC top plate.

3.6. Optical readout

The light produced in the scintillator is collected by wavelength shifter plates (WLS) located on both sides of a module. This two-sided readout of the scintillator provides redundancy and improves the homogeneity of the response in azimuth. The WLS used for the ZEUS barrel calorimeter is PMMA (polymethyl methacrylate) doped with 30 ppm of fluorescent dye Y-7 [7]. The thickness of the WLS plates is 2 mm which allows 32% of the light to traverse the plate without being absorbed and shifted.

To correct for the different light yields of the scintillator tiles in a given tower, for the thicknesses of the DU plates and for the variation in the light collection efficiency within a WLS plate, a varying fraction of the light traversing the WLS unabsorbed is reflected back into the WLS. This is achieved by backing the active area of the WLS plates with reflective aluminum masks having printed patterns of black stripes. The mask

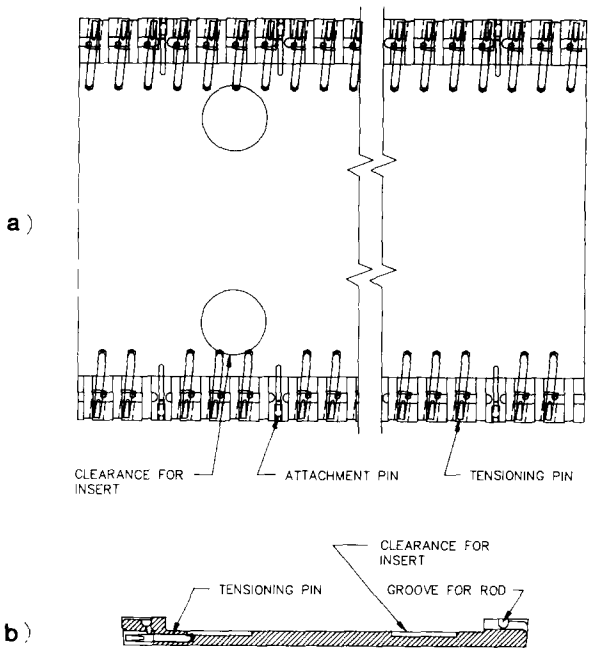

Fig. 10. Details of the EMC top plate: (a) top view; (b) cross section.

patterns were individually produced, based on measurements of the light output of each scintillator piece, the thickness of each DU plate at the location of a

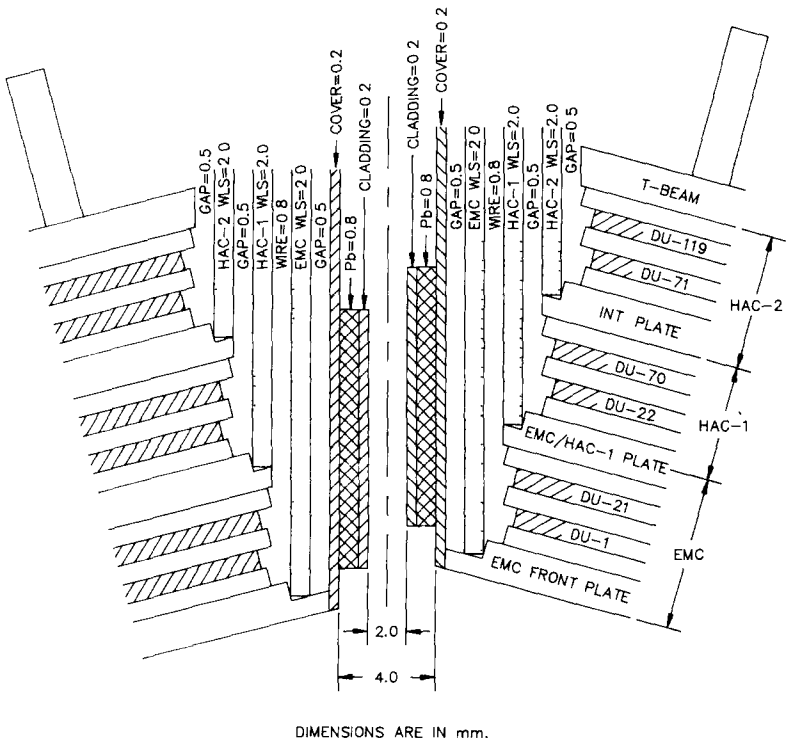

Fig 11. Dimensions of the intermodule gaps.

given piece of scintillator and the light collection efficiency of the WLS mapped over its active area.

The WLS plates also guide the light from the scintillator to the photomultiplier tubes (PMTs) located at the back of each module, see figs. 4 and 5. The plates for the three different sections of a given tower lie on top of each other, as shown in the schematic of fig. 11. The WLS plates for the HAC_{II} are covered by the plates for HAC_{I}, which in turn are covered by the plates for the readout of the EMC section.

The WLS guides are coupled to the PMTs via a cylindrical transition piece made of the same material. The attenuation length in the WLS being of the order of 1 m, the light loss in transmission is sufficiently small to justify the use of the same material as light guide, so avoiding the inevitable nonuniformities coming from the use of glue joints.

3.7. Calibration tools

Measurement of the energy of particles involves the following steps:

a) light production in the scintillator;
b) light transmission to the WLS;
c) wavelength shifting in the WLS plate;
d) guidance of the light to the transition piece;
e) transmission to the PMT;
f) photoelectron production in the photocathode of the PMT;
g) photoelectron multiplication by the PMT;
h) analog signal processing by the front end electronics;
i) digitization by analog-to-digital converters.

Three calibration tools are provided to monitor the performance of the above chain of processes a)–g): DU current measurements, ^{60}Co source scans and pulsed laser light injection.

The natural radioactivity of the DU generates a constant level of light in the scintillators for integration periods of a few ms. This light is manifest as an enhanced dark current of the PMTs, called the DU current. The initial calibration of the calorimeter is done by adjusting the gain of the PMTs to yield specific values of the DU currents. These values (156 nA for the EMC, 838 nA for the HAC_{I} and 1106 nA for the HAC_{II}) are determined by the total area of scintillator exposed to DU, the attenuation length in the scintillator and the thickness of the stainless steel cladding of the DU plates. Once the gains are set, the DU current is constantly monitored to reveal any changes in the efficiencies of steps a) through g) in the above list.

The light production of each piece of scintillator, the transmission to the WLS and light shifting efficiency of the WLS including its mask were tested by moving a ^{60}Co source along the edge of the calorimeter. There are 26 stainless steel tubes, each with a 2 mm outer diameter, positioned along each side of the module, one between every other WLS of the EMC. These tubes run from the T-beam to the front plate of the EMC and are accessible at the end protruding beyond the T-beam. The ^{60}Co source was attached to the tip of a piano wire which was inserted into the tube and driven by two rubber wheels coupled to a stepping motor [7].

The characteristics of the PMTs, i.e. the photoelectron efficiency, gain and linearity, were measured and monitored by a UV dye laser light system [8]. The laser flasher system injects light into the transition piece in front of each of the 162 PMTs of a module. The optical fiber distribution system is placed in the T-beam region; the light sent to a module is divided twice to feed two 1:90 splitters which, in turn, feed 81 channels on each side of the module. The laser calibration system and the analog part of the readout system located on the T-beam were provided by our collaborators from Pennsylvania State University and Columbia University, respectively.

The front end and digital electronics, i.e. steps h) and i), were calibrated, independently of the optical system, by a charge injection system that allowed an injection of specific charges into the inputs of the analog cards.

3.8. Intermodule gap

Fig. 11 shows a schematic of the azimuthal gap between modules. The total distance between scintillator tiles is 11 mm for the adjacent EMC sections and 16 (21) mm for the HAC_{I} (HAC_{II}) sections. The size of the scintillator tiles is chosen such that their ends protrude by 0.5 mm beyond the DU, since a small overhang of the DU plates would cause significant losses in the light collection by the WLS plates.

To reduce the production of Cherenkov light generated by electromagnetic showers in the wavelength shifters and so to flatten the response to electrons incident close to the intermodule boundary, the module covers are made of 0.8 mm lead sandwiched between two 0.2 mm stainless steel sheets. This lead sandwich covers the whole surface of the EMC and HAC_{I} and reduces the nominal space between modules in this region from 4 to 2 mm.

The effect of the lead is negligible for incident hadrons, but dramatically improves the homogeneity of the response to electrons and photons. Without lead the response, measured as the sum of the two neighbouring modules, increases by as much as 35% for electrons incident close to the crack, despite the 2.5° azimuthal tilt of the modules. Beam tests at CERN [3] and FNAL [9] showed that with the inclusion of about 2 mm of lead between modules the response can be

made flat to ±5% when scanning across the crack. These results were corroborated by detailed simulation studies of electromagnetic showers generated by electrons and photons incident on the intermodule boundary [6].

4. Fabrication of components

The components required for the assembly of the BCAL modules were fabricated by industrial companies in conjunction with the collaborating US universities and Argonne National Laboratory (ANL). The components were shipped directly to the two assembly sites: to ANL and, for the sections assembled in Germany, to the Kernforschungsanlage (KFA) Jülich.

4.1. Fabrication of DU plates

The DU was provided in the form of 651 billets, each weighing about 830 kg, by Martin Marietta Energy Systems, Oak Ridge, TN, USA. The billets contained 1.4–2.0% of Nb by weight and the carbon content did not exceed 440 ppm by weight. Specifications limited the maximum content of ^{235}U to 0.3% [10]. A chemical analysis was performed on every billet.

Of the 119 DU plates comprising a module, 21 are used for the EMC section, while the remainder are divided equally between HAC_I and HAC_{II}. Table 2 lists the nominal dimensions of the DU plates. The length of plates 29 through 119 remains constant. Since the plates increase linearly in width for the HACs only the dimensions of the first and last plates of each

Table 2
Dimension of DU plates

Section	Plate number	Length [mm]	Width [mm]
EMC	1	2694.75	234.29
	2	2711.99	235.87
	3	2729.23	237.45
	4	2785.25	242.57
	5	2802.49	244.14
	6	2819.73	245.72
	7	2836 97	247.29
	8	2854.21	248.87
	9	2871.44	250.45
	10	2888.68	252.02
	11	2905.92	253.60
	12	2923 16	255.17
	13	2940.40	256.75
	14	2957.63	258.33
	15	2974.87	259.90
	16	2992.11	261.48
	17	3009.35	263.05
	18	3026.59	264.63
	19	3043 83	266.20
	20	3061.06	267.78
	21	3078.30	269.36
HAC_I	22	3158.21	271.64
	23	3175.88	273 25
	24	3193.55	274.87
	25	3211.22	276.48
	26	3228.89	278.10
	27	3246 56	279.71
	28	3264.23	281.33
	29	3270 23	282.94
	.	:	:
	70	3270.23	349.17
HAC_{II}	71	3270.23	350.20
	:	:	:
	119	3270.23	427.74

sequence containing plates with identical length are displayed in table 2. The nominal thickness for all plates is 3.3 mm, or $1X_0$. Fig. 12a shows a compilation of all measurements on a set of plates from a given module. The measurements were done at three points (left, middle and right) across the plate for 27 (52) locations along the length of the HAC (EMC) plates. In fig. 12b the differences between the left and the right measurements are displayed, indicating a very slight asymmetry. Finally, fig. 12c shows the average of all measurements for a set of plates versus module number. The error bars were calculated as the variance of the measurements.

Both the HAC and the EMC plates are rectangular in shape. The HAC plates, however, have two additional features, as shown in fig. 7a. The plates have rectangular keyways cut out at the two ends to accommodate the keys of the end plates and end plate extensions and they feature 13 pairs of slots to allow for the insertion of the tensioning straps.

The plates were produced by Manufacturing Sciences Corporation (MSC) of Oak Ridge, TN, USA.

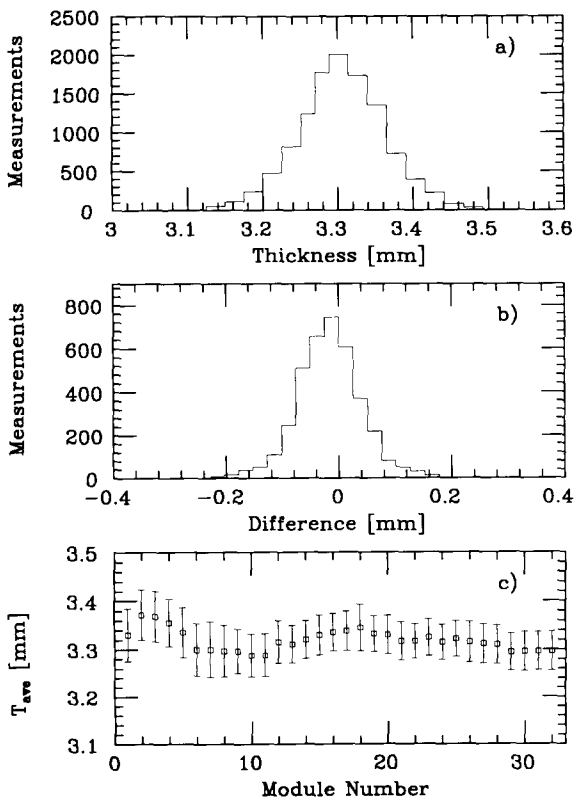

Fig. 12. Thickness measurements of the DU plates: (a) all measurements for the plates of a typical module; (b) difference between the measurement on the left and the right edge of the plates of a typical module; (c) average of all thickness measurements vs module number.

Table 3
Specification of tolerances for DU plates

Section	Maximum deviation of any single measurement from the nominal value [mm]		
	thickness	length	width
EMC	0.25	0.25	0.51
HAC_I	0.25	0.51	1.02
HAC_{II}	0.25	0.51	1.02

Strict restrictions on the acceptable variations in dimensions, flatness, edge straightness and the location of the keyways and slots were imposed, as summarized in table 3. Details on the other requirements may be found in ref. [10].

The dimensions of all plates were carefully measured and checked to satisfy the tolerance specifications. The thickness was measured either using a semi-automatic system at ANL or a fully automatic system at MSC. The latter was developed by the Canadian institutions responsible for similar measurements on the DU plates for the forward and rear calorimeters. The thickness measurements were further used as input for the production of the patterns on the WLS masks and in the selection of the spacer height to be used in the stacking operation. The length and width measurements together with the slot and keyway locations relative to the plate center line and front lateral edge were checked by laying the plate on a specially constructed gauge plate. Finally, the plates were weighed and checked for flatness, twist, camber and lateral bow.

4.2. Cladding of DU plates

The purpose of cladding the DU plates in stainless steel sheets is threefold. First, it reduces the irradiation of the scintillator from the natural radioactivity of the DU to the appropriate level. Considerations of the dark current and the lifetime of the PMTs established the appropriate cladding thickness to be 0.2 (0.4) mm for the EMC (HAC) plates. Measurements on the PMTs show that the gain drops by a factor of two for a total collected charge of 200 C. This corresponds to seven years of continuous operation at a current of 1 μA. Secondly, it reduces the radiation doses to which the technicians were exposed during the assembly of the modules by about an order of magnitude. A typical dose rate at the surface of a clad plate is 0.1 mSv/h. Thirdly, it prevents the possible spread of uranium oxide into the calorimeter during the stacking operations and over the lifetime of the experiment. In this regard, the addition of Nb to the DU significantly reduced the rate of oxidation.

Fig. 7b shows the cross section of a clad DU plate. For the HAC plates the cladding parts consisted of four 0.2 mm sheets and six 0.2 mm U-channels of stainless steel which completely enclose the edges of the plate except for the keyways at the ends, whose faces are the only parts of the DU plate exposed to air before stacking of the modules.

The EMC plates used four 0.1 mm sheets and four 0.075 mm U-channels as shown in fig. 7c. The reduced thickness of the cladding steel required the addition of a 12.7 mm wide band of niobium under the welding spots. The thickness of the band is 0.025 mm and it acted as a barrier to prevent penetration of DU into the weld with subsequent reduction in weld strength. This technique was also applied on the plates for the HAC sections of eleven modules.

The steel sheets were provided by Teledyne-Rodney Metals, Maryland Heights, MO, USA. The thickness tolerance was better than ± 2.5 μm. The sheets were cut, punched (the slots for the HAC plates) and formed (the U-channels) by Held Metalcraft Inc., Chicago, IL, USA.

The cladding sheets and U-channels were manually welded at spaced intervals to form a tight and sturdy box around the DU-plates using a direct-current condenser-discharge spot-welder. The slots in the HAC plates were covered with grommets set in the slots by a grommet setting tool. The cladding welds were very strong, so that the plates could be handled safely by a vacuum lifter with suction cups. The entire cladding operation was performed at ANL.

4.3. Scintillator

The scintillator used for the calorimeter is SCSN-38, manufactured by Kyowa Gas Chemical Inc., Tokyo, Japan. The material consists of a cross-linked polystyrene base doped with two wavelength shifting dyes: butyl-PDB (1%) and BDB (0.02%). This particular choice was based on the high light output, the long attenuation length, the stability when exposed to air over long periods of time and the extensive experience gained in other high energy physics experiments. The scintillator was purchased in large sheets of 2.6 ± 0.07 mm thickness and laser cut into tiles by Laser Services Inc., Westford, MA, USA [7].

The total number of pieces in the entire BCAL is 82112: there are 22 (300) different sizes in the EMC (HAC) section. Table 4 summarizes the different sizes of scintillators used. In the EMC all pieces in a given layer are identical in size, but the projective geometry and the wedge shape of the modules required that the pieces increase both in width and length with increasing distance from the beam axis. Due to the nonprojective geometry in the HAC, the width of the pieces remains constant for all pieces in all towers except for the pieces in the first seven layers of the first and last HAC_I towers, see fig. 4. However, because of the

Table 4
Summary of scintillator tile sizes

Section	Layer	Towers					
		first		remainder		last	
		width [mm]	length [mm]	width [mm]	length [mm]	width [mm]	length [mm]
EMC	1			49.20	234.45		
	:			:	:		
	4			50.17	239.15		
	5			51.23	244.28		
	:			:	:		
	22			56.76	271.07		
HAC_I	23	147.75	271.83	227.91	271.83	186.08	271.81
	24	158.75	273.43	227.91	273.43	192.76	273.43
	25	169.75	275.03	227.91	275.03	199.42	275.03
	26	180.75	276 66	227.91	276.66	206.10	276.66
	27	191.77	278.28	227.91	278.28	212.75	278.28
	28	202.77	279.88	227.91	279.88	219.43	279.88
	29	207.39	281.51	227.91	281.51	225.50	281.51
	30	207.59	283.11	227.91	283.11	225.50	283.11
	:	:	:	.	:	:	:
	72	207.59	350.95	227.91	350.95	225.50	350.95
HAC_{II}	73	207.59	350 14	227.91	350.14	225.50	350 14
	:	:	.	:	:	:	:
	122	207.59	429.29	227.91	429.29	225.50	429.29

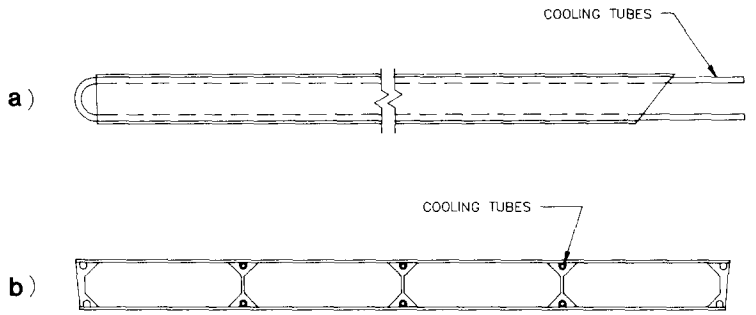

Fig 13. The HES box: (a) side view; (b) cross section.

wedge geometry, the length increases linearly with distance from the beam axis. As previously noted, the scintillator pieces for the outer towers are narrower.

After cutting, the scintillator tiles were washed and individually wrapped in a 0.05 mm mirror finished aluminum foil. The wrapping improves the uniformity of the optical response along the length of the tiles and protects the scintillator from dirt and dust during the assembly operations. In addition, to reduce the enhanced light output at the ends, the two ends are wrapped in 30 mm wide stripes of black Tedlar. With these wrappings the light response from the center of the tile to the ends was uniform to within ~ 5% [7,11].

The wrapped scintillator pieces were scanned by a 0.4×10^6 Bq ^{106}Ru source on a CAMAC driven X–Y scanning table. Each piece was measured at five different locations and the data were used as input for the production of the WLS mask patterns. The design and production of the optical system were the responsibility of our collaborators from the Ohio State University and from the Louisiana State University.

4.4. Box for the hadron–electron separator

To enhance the electron–hadron separation and to improve the position resolution for photon induced electromagnetic showers we intend to implement a fine grained detector, the hadron electron separator (HES), at the approximate depth of the maximum of electromagnetic showers. Two detector technologies are currently under investigation: silicon pads [1] and scintillator pads with fiber readout. As a pilot program the RCAL will be equipped with a partial HES using 30×30 mm^2 silicon pads for the first ZEUS data taking period. The remainder of the calorimeter is planned to be equipped with an HES by 1992–93.

In order to accommodate the HES in the BCAL an aluminum box is built into the EMC section after the 4th layer of scintillator. Fig. 13 shows the side view and the cross section through this box. It is open at the rear end, so that, at the time of the upgrade, the detectors may be slid in without disassembly of the modules. The box is strengthened by ribs which contain stainless steel

Table 5
Suppliers of parts for the HAC box

Item	Number	Supplier
T-beam	6	Alumni Tools & Die, South Bend, IN, USA
	26	Hans Schlaak Maschinenbau, Osnabrück, Germany
Holey plates	32	PSL, Univ. of Wisconsin, Madison, WI, USA
End plates	4	Alumni Tools & Die, South Bend, IN, USA
	28	Hans Schlaak Maschinenbau, Osnabrück, Germany
End plate ext.	32	Nevis Labs., Columbia Univ., Irvington-on-Hudson, NY, USA
Intermediate plates	4	Alumni Tools & Die, South Bend, IN, USA
	28	Hans Schlaak Maschinenbau, Osnabrück, Germany
Front plates	6	Alumni Tools & Die, South Bend, IN, USA
	26	Hans Schlaak Maschinenbau, Osnabrück, Germany
Straps	32×26	ANL, Argonne, IL, USA
Spacers	50%	Standard Grinding & Manufacturing, Skokie, IL, USA
	50%	Production Milling Works, Melrose Park, IL, USA
Inserts	6×52	Monnett Precision Grinding, Addison, IL, USA
	26×52	GMZ Blank, Utersen, Germany

tubes of 2.4 mm diameter to allow for water cooling of the electronics mounted on the boards of the silicon pad detectors. The two steel tubes in a given rib are connected by a U-shaped tube at the front end. The connections to the water supply and return are made at the rear end. Prior to installation in a module and after completion of a module, the tubes were tested with compressed air at pressures up to 1.7×10^6 Pa to ensure freedom from leaks.

The aluminum ribs were fabricated by Production Milling Works, Melrose Park, IL, USA and part of the HES boxes were assembled at ANL and part by Ideal Tool Inc., Chicago, IL, USA. Special care was taken to maintain the nominal dimensions to an accuracy of ± 0.25 mm.

4.5. Support structures for the HAC

Table 5 lists the suppliers for the support structures of the HAC. Most components are made of iron: exceptions are the holey plates and the end plate extensions which are made of aluminum and the rear end plates which are made of austenitic stainless steel. The T-beam, the intermediate plate and the end plate in the forward direction use ferromagnetic iron to reduce the magnetic forces experienced by the solenoid. However, for the first four modules constructed, the intermediate plate and the end plate in the forward direction were made using stainless steel. These modules will be installed into the ZEUS detector at 45°, 135°, 225° and 315° from the vertical.

The holey plates are bolted to the T-beam and serve as locators for the upper end of the WLS light guides and as support for the magnetic shields of the PMTs, the front end electronics and the upper half of the module side covers, see figs. 4 and 5.

The straps, which are made from 1075 high carbon steel, were heat treated to increase their strength. In repeated tests the straps yielded at tensions ~ 5.5 tons, as compared to the tension applied during compression of the HAC of ~ 3 tons. Slotted inserts are used in the base of the T-beam and the other plates. Ease of manufacture and cost considerations imposed this solution in preference to the direct cutting of slots in the steel plates.

4.6. Support structures for the EMC

Table 6 lists the suppliers for the support structures for the EMC. The top plates, front plates, end frames and spacers are all made of aluminum. The top plate, shown in fig. 10, has an intricate design since it must accommodate the tuning pins, the rods to hold the wire loops and the pins to attach the EMC to the HAC section.

The tuning pins are a modified version of pins used for autoharps and were made of 4140 carbon-steel, heat treated to increase their strength. The pins typically break at torques exceeding 15 N m which is an order of magnitude above the maximum torque applied by the wires. The pins were inserted at an angle of 5° into the top plate in order to leave their ends accessible to the tuning hammer and away from the wires.

The wires are held at one end by a loop around a stainless steel rod embedded into the EMC top plate. To make the loop the wires are passed three times through a small copper ferrule which prevents them from slipping even at the maximum wire tension of ~ 64 kg.

4.7. Optical readout

The WLS material was procured from Kyowa Gas Chemical Company, Tokyo, Japan in the form of 1.86 m^2 sheets. The nominal thickness is 2 mm and variations up to ± 0.4 mm were accepted. These WLS sheets were laser cut to produce 53 different shapes for the EMC and three for each HAC section by Laser Services Inc., Westford, MA, USA. After cutting, the WLS plates were washed and annealed at 82°C. Fig. 14 shows a sketch of both an EMC and an HAC WLS. Before forming the fingers into a bundle and bending the HAC WLS near the top, the WLS plates were heated in an oven. After bending, the bundles were cut off and machined to the correct length and the WLS were reannealed. Finally, the WLS were carefully

Table 6
Suppliers of parts for the EMC box

Item	Number	Supplier
Rear plate	32	ANL, Argonne, IL, USA
Tuning pins	20%	ANL, Argonne, IL, USA
	80%	Arrow Screw Engineering, St. Charles, IL, USA
End frames	32	Nevis Labs., Columbia Univ., Irvington-on-Hudson, NY, USA
Front plate	32	ANL, Argonne, IL, USA
Wire	100%	Elgiloy Limited Partnership, Elgin, IL, USA
Wire loops	20%	Paraplegics Manufacturing Comp., Bensenville, IL, USA
	80%	Consolidated Manufacturing, Monee, IL, USA
Spacers	100%	Production Milling Works, Melrose Park, IL, USA

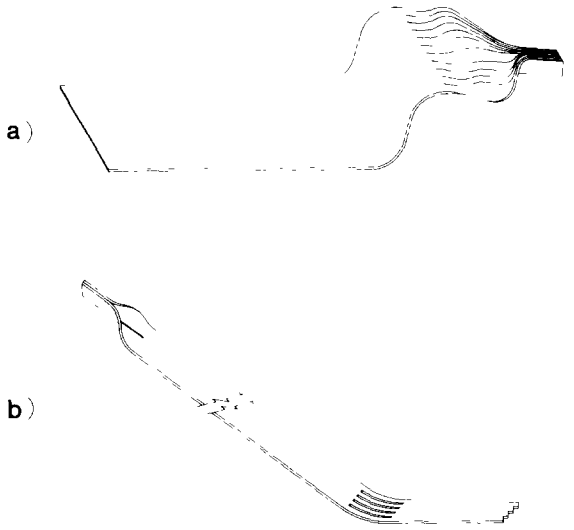

Fig. 14. Examples of the WLS plates for (a) an HAC and (b) an EMC tower.

washed and the unexposed areas wrapped in aluminum foils.

The light output from each WLS light guide relative to a standard one was measured by exposing both to a UV lamp. Approximately 2% of the WLS light guides were rejected due to poor light output. The WLS masks were produced by transferring the computer generated patterns to acetate film using a TI-3000 laser printer which in turn was imaged onto Dynamark. Details of the WLS and mask fabrication can be found in ref. [7].

The total number of PMTs for the BCAL is 5184. The Hamamatsu R-580 10-stage PMT was selected for both the HAC and EMC sections based on requirements of dark current, noise and gain characteristics. The following properties of each PMT were measured:
a) photoelectron efficiency;
b) gain as function of high voltage;
c) rate effects;
d) gain stability; and
e) dark current.
In addition, selected PMTs were tested in long term lifetime measurements. The acquisition and testing of PMTs was the responsibility of collaborators from the University of Wisconsin.

Safety considerations connected with the DU precluded the use of conventional resistive bases driven by high voltage supplies located outside of the detector. A solution that avoids these hazards generates the high voltage within the base for each PMT using a small Cockcroft–Walton voltagedoubler (CW) [12]. This CW base consists of a 100 kHz oscillator powered by a 24 V dc power supply, a ferrite transformer and a chain of rectifiers and capacitors. The power consumption for such a base is low, $P \approx 0.12$ W. The design, production and testing of the 5184 bases required was done by collaborators from the Virginia Polytechnical Institute and State University.

4.8. Module side covers

The module side covers are made from 0.2 mm stainless steel sheets. Each cover is split into two parts, the lower one covering the EMC and HAC_I and the other the HAC_{II} section. They are joined by a C-shaped clip which runs along the whole length of the module. To improve the homogeneity in azimuth for electromagnetic showers located close to an intermodule gap, a sheet of 0.8 mm lead is bonded to the lower side cover with a sheet of 0.2 mm stainless steel bonded to its outer surface, making a sandwich. The whole cover weighs approximatively 30 kg per side and is connected to the end plates, the EMC front plate and the holey plate by a set of 198 screws. The side covers are in slight tension and to maintain a light tight environment in the module the edges were covered with aluminum tape. The covers were fabricated by MLW Products, Inc., Chicago, IL, USA.

5. Assembly of the modules

The module assembly was done in three steps: a) the HAC section stacking, b) the EMC section stacking and c) the assembly of the optical readout and the installation of the module covers. Both steps a) and c) were carried out at KFA as well as at ANL. All tools, fixtures, jigs etc. needed for the assembly of the modules at KFA were duplicates of the equipment used at ANL and were constructed in the USA.

5.1. Stacking of the HAC section

Fig. 15 shows a photograph of the stacking fixture used for the assembly of the HAC sections and also for mating the EMC and HAC sections. The entire fixture can be raised and lowered to keep the top of the stack at a comfortable working level. The assembly procedure started by setting the HAC box consisting of a T-beam, a front plate, end plates and end plate extensions on the fixture. The end plates were bolted to trunnions which sit in U-shaped supports allowing the finished module to be picked up by the crane or to be raised or lowered by the hydraulic system of the stacking fixture. The latter option was necessary for the insertion of the tensioning straps and also during the mating operations. The trunnion support also allowed for the rotation of a completed stack to selected orientations.

The box was anchored to the fixture and carefully aligned by an optical survey to a typical accuracy of 0.4 mm. After alignment the T-beam was removed for access in stacking.

The stacking operation, which was straightforward, was performed manually. Using a locating jig, a set of three spacers was glued down at the gaps between scintillator tiles. The spacers were specified by a computer program using the thickness measurements of the DU plates as data base. To prevent the scintillator from moving, 3×3 cm^2 one sided adhesive foam pads were laid on the front plate close to the four corners of the scintillator tiles. The fourteen pieces of scintillator were laid down and their four corners were similarly covered with foam pads. The first DU plate was placed on top of the spacers using the vacuum lifter. Its lateral location was defined by the keys in the end plates and end plate extensions. The plates were aligned in the longitudinal direction by means of a feeler gauge inserted in the gap between the key of the front end plate and the DU plate. As a check of the slot alignment, after every few plates a tensioning strap was inserted into the 26 slots of the DU plates.

This procedure was repeated for the 50 layers of HAC_I and completed by placing a final 1.8 mm stainless steel shim before the intermediate plate. After laying the intermediate plate on top, the stack was compressed by an hydraulic system to a pressure of 14.5×10^6 Pa. The stack height was carefully measured at ten locations, five on each side. Fig. 16a shows a typical example of such a measurement. If the deviations to the nominal values exceeded 0.75 mm additional shimming was used and the new stack height measurements were employed as input for a revised calculation of the spacer list for the HAC_{II}. Since the patterns on the WLS masks for a given scintillator layer cover the space from the middle of the DU plate below to the middle of the DU plate above, considerable deviations in the stack height from layer to layer were permissible.

HAC_{II} was stacked in exactly the same way. The stack was completed by setting the T-beam on top and was again compressed hydraulically. Fig. 16b shows the height measurements for a completed stack of a typical module. The stack heights were in general short by up to 1 mm. This was corrected by a stainless steel shim introduced between the last layer of scintillator and the T-beam. After shimming the stack height was remeasured, see fig. 16c.

Finally, the compressed module was raised by the hydraulic system of the stacking fixture and rotated 45° on the trunnion supports with the help of the

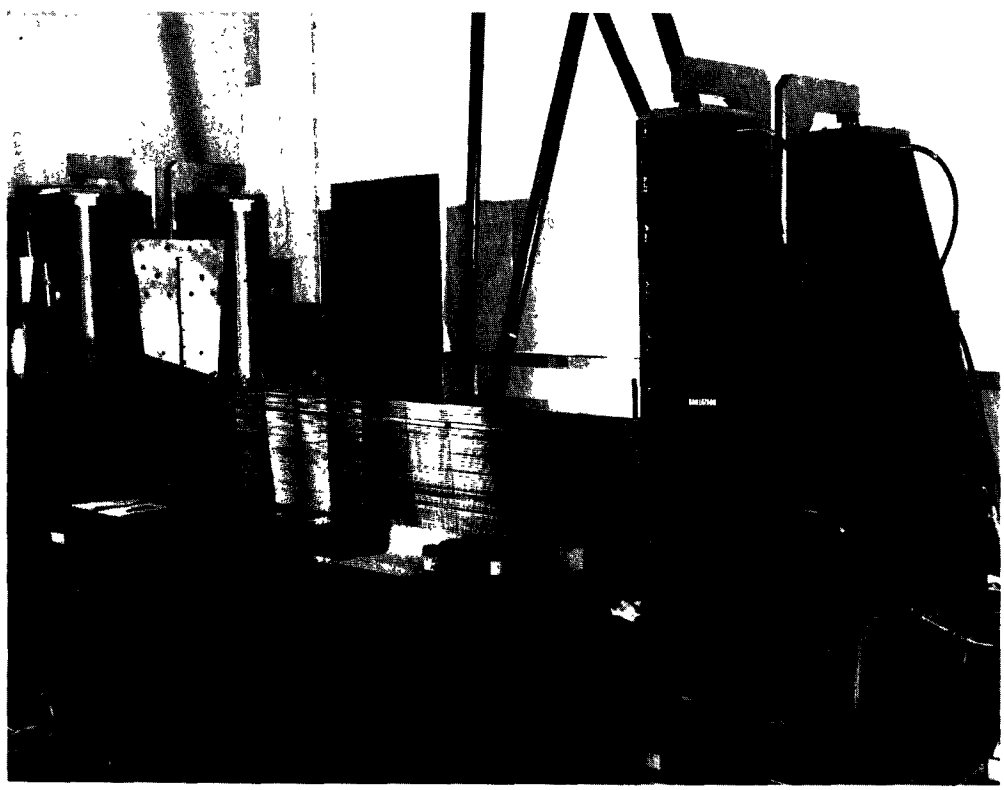

Fig. 15. HAC stacking fixture with a partially stacked module.

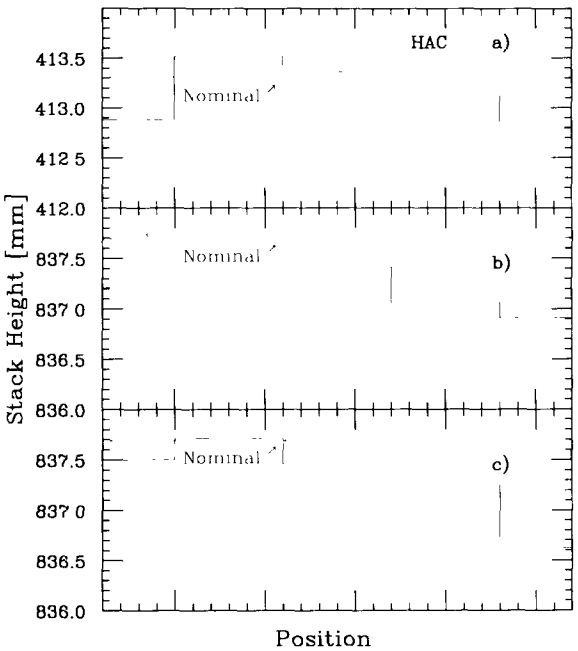

Fig. 16. Typical HAC stack height measurements: (a) at the intermediate plate, (b) of the complete stack before shimming, and (c) of the complete stack after shimming.

overhead crane. After insertion of the straps from the bottom, the module was made vertical and set onto the stacking fixture. The strap assemblies were completed and the straps individually tensioned using an hydraulic bolt tensioner. The nominal overall compression was 20.7×10^6 Pa.

5.2. Stacking of the EMCs

The EMC sections were stacked in a separate clean room independently of the HAC stacking operation. Fig. 17 shows the EMC stacking table with a completed EMC section under compression. The assembly procedure started with the setting up of the EMC box, consisting of the front plate and the two end frames, onto the stacking table. The first layer of scintillator, with each piece being separated by an aluminum spacer, was laid on the front plate. The location of the spacers was determined by grooves machined in the front plate. A 3×3 cm^2 foam pad at the center prevented each scintillator piece from moving. The first DU plate was laid on top of the spacers and aligned lengthwise by comparison with machined groves in the end frames. The sideways alignment was performed by adjusting the plate position so that the gaps between the plate

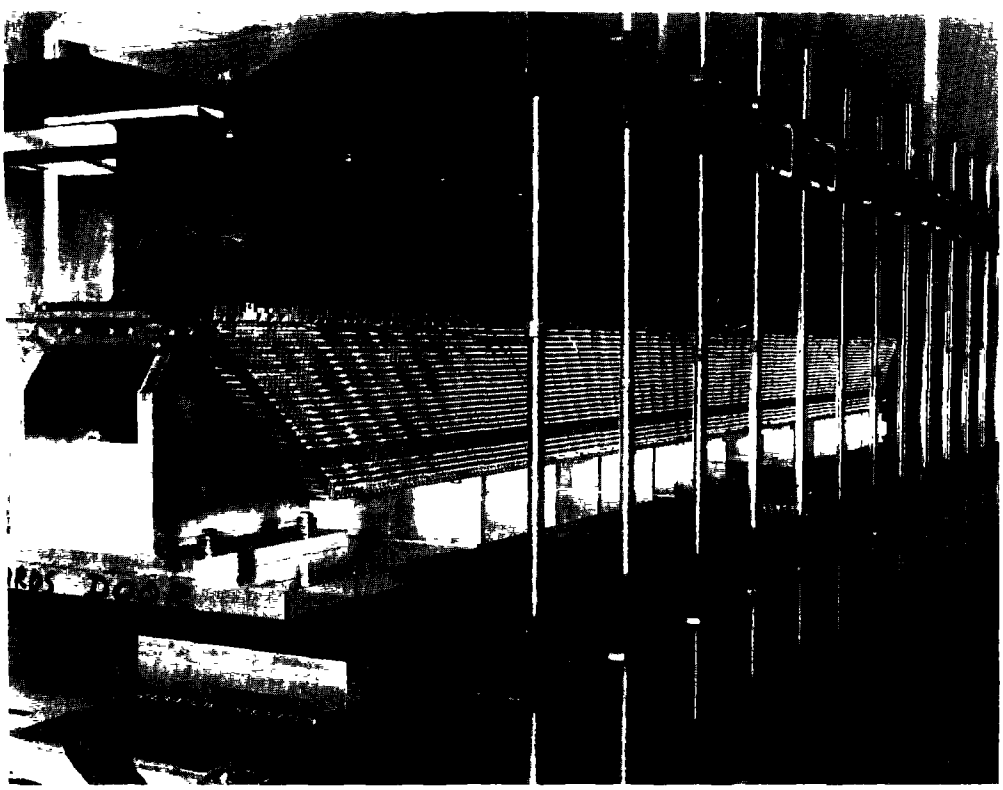

Fig. 17. The EMC stacking fixture with a completed section under compression.

and the capturing lips of the end frames were equal on both sides. The next layers were stacked in the same way as the first except for the application of additional foam pads which were glued on the DU plates under the center of each scintillator piece.

In the projective towers the scintillator pieces grow in width with successive layers. This required all the spacers for a given layer to be glued equidistantly, but at a different distance than that for any other layer. A special fixture, that was reset for every layer, was used to glue the spacers at their required location. Every other spacer of a layer was glued to the stainless steel cladding using this fixture and the two corresponding scintillator pieces and the spacer in between the two glued spacers were slid in from the side. After the fourth layer of scintillator the HES box was inserted. Its alignment was adjusted in a similar manner to that used in positioning the DU plates.

The stack was completed with a 0.5 mm stainless steel shim between the last layer of scintillators and the top plate. The shim extended over the whole length of the EMC and primarily served to protect the last scintillator layer from damage during the wire mounting operation. The completed stack was compressed with a force of ~3 tons using a set of 13 box beams under and above the stack with threaded rods connecting them. The top beams were mounted on a steel I-beam running the length of the module, as seen in fig. 17. The stack height was measured at twelve locations on each side. The measurements of a typical module are displayed in fig. 18a.

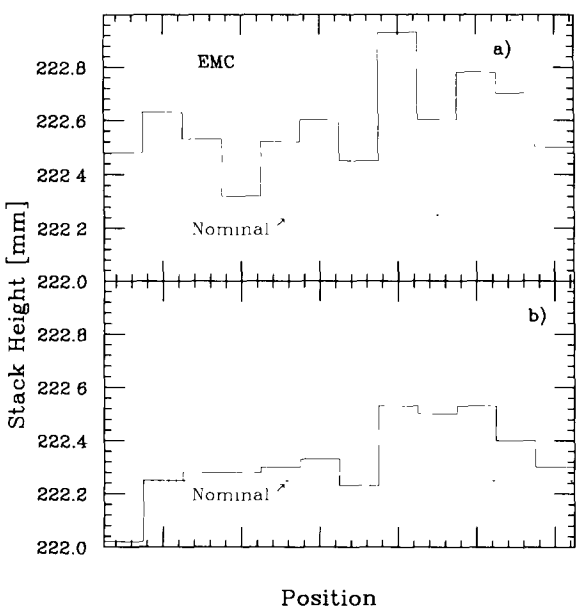

Fig. 18. Typical EMC stack height measurements: (a) before and (b) after tensioning of the wires.

While keeping the stack under compression the wires were mounted and tensioned. The wires are alternately held on one end by a loop around a stainless steel rod and tensioned at the other end by a tuning pin. The final wire tension was obtained in several iterations in which the wires were first pulled by a hook to the side of the tensioning pin and then retensioned. The wires were pulled in order to overcome the friction on the two corners of the front plate and, therefore, to increase the tension of the wire on the side of the loop. Typically a dozen wires per module snapped during the tensioning procedure. The break occurred either while pulling at one of the corners of the front plate or while tensioning at the point of maximum tension, between the tuning pin and the first bend of the wire. The broken wires were replaced and tensioned to the nominal tension.

After tensioning the wires the compression fixture was taken off and the stack height was remeasured, see fig. 18b. The variance in height was typically within ± 0.4 mm of the nominal value. The stack compressed in average by 0.25 mm between the initial external compression and the final compression by the tensioned wires.

The completed EMC sections were secured with nylon straps to a rigid steel I-beam and set on the HAC stacking fixture for mating with the HAC sections. To facilitate the relative alignment of the two sections the EMC was laid on sheets of bearing material. The mating operation has been described above.

5.3. Assembly of the optical readout components

The optical readout components were installed in a separate clean room, independently of the stacking activities. The module, supported by trunnions, was held in a frame which allowed it to be rotated to a horizontal position so as to facilitate the installation of the WLS light guide system.

The holey plates for the support of the WLS guides, the PMTs and the front end electronics were first mounted one on each side of the T-beam. In order to create a light tight cavity in the T-beam below the holey plate, all seams between the holey plate and the T-beam were closed from above and below by a filling of black RTV. The laser splitter and optical fiber system was then installed in this cavity and bolted to the web of the T-beam.

The scintillator tiles were carefully inspected and any wrapping material protruding beyond the ends was cut off with a razor blade. To avoid shadowing of the ends by the DU plates the scintillator tiles were again laterally centered by laying an aluminum plate, constrained to occupy the plane of the WLS, over the scintillator.

The WLSs were mounted one side at a time, first the HAC_{II}, then the HAC_{I} and, finally, the EMC. The WLSs were positioned, so that the layer structure of the mask patterns was properly aligned with the corresponding layers of scintillator. The HAC WLSs are held in place by tape and by clips attached to the T-beam and intermediate plate with teflon spacers inserted between adjacent guides. The EMC WLSs are taped down to the underlying HAC WLS and also held by brass bands running between the scintillator pieces and spacers of the last EMC layer. The brass bands were tightly pulled and soldered together. After installing the WLSs and connecting up all the light fibers, the integrity of each optical path was checked visually using an incandescent source. The ^{60}Co source tubes were installed between every other EMC WLS and secured with adhesive tape.

Finally, the module's sides were protected by covers of stainless steel. The covers are installed as two parts, the upper part covering the HAC_{II} and the lower with the additional 0.8 mm lead sheet covering the HAC_{I} and EMC sections. The two parts are joined by a C-channel clip and secured to the module by screws. To ensure light tightness the boundaries of the cover were covered with aluminum metal tape and/or RTV.

6. Tests of mechanical properties

6.1. Measurements on the HAC

In addition to a number of tests using small stacks [13], the mechanical properties of the HAC were studied on both a prototype HAC section stacked with steel plates and a full size prototype module using DU plates [14]. In the case of the steel plate stack the weight of the DU plates was simulated by lead sheets inserted into the gap normally occupied by the scintillator tiles. The weight of the EMC was simulated by attaching the appropriate amount of lead to the HAC front plate. The dimensions of both prototypes differed very slightly from the dimensions of the production modules.

The response of the module to a longitudinal shear force was measured with dial indicators placed against one of the end plates at the height of the front plate of the HAC sections. The shear forces were applied with a hydraulic cylinder pushing against the opposite end plate at the same height. The stacked module was strong in shear: the deflection being ~ 0.5 mm/ton of force. The overall structure including the spokeswheels is stronger than that of 32 unsupported modules. The combined force exerted on the installed modules by the magnetic field and the overall 0.4° tilt of the ZEUS detector is estimated to be 7.7 tons.

The deflection of the front plate both in the vertical and horizontal orientation of the module was measured, i.e. before and after a 90° rotation of the module around its longitudinal axis. The deflections did not exceed 0.5 mm.

During the tensioning of the straps, the 90° rotation of the modules and the longitudinal shear tests, the stresses on the straps and the module structure were monitored using strain gauges. Applying the nominal tension to the straps resulted in a stress about 70% of yield. Although the expected stresses on the module are low, strain gauges were mounted throughout the structure to check the load sharing. All stresses recorded during the strap tensioning and subsequent rotation of the modules were well below the shear strengths of the appropriate materials.

As a check the mechanical properties of the modules were calculated using the ANSYS finite element program. The modules were simulated both by two and three dimensional models [15]. The results were in reasonable accord with the measurements.

6.2. Measurements on the EMC

The mechanical properties of the EMC section were investigated with a 26 cm long test section [16]. The test section used steel plates clad in stainless steel sheets and brass or aluminum spacers. The section was held together by wires in a similar way to the production modules.

The mechanical deflections of the test section were measured after rotation by 90° and subsequent loading with lead sheets to simulate the weight of the DU. In the final configuration that used aluminum spacers and welded cladding sheets, the deflections for the fully loaded test section did not exceed 0.5 mm. They did not increase with time over a period of 30 days during which the test section was left with the plates vertical.The stresses in the end frames were measured with strain gauges mounted on the completed prototype stacked with DU plates. The maximum stress recorded during rotation by 90° was more than an order of magnitude below the yield stress of aluminum.

The deflection of the EMC section mounted on the DU prototype was measured in an optical survey. The measurements taken with the module both in the vertical and horizontal positions do not allow an unambiguous disentanglement of the observed deflection due to the HAC or the EMC section. If most of the effect is attributed to the EMC section its deflection is about 0.5 mm. For the production modules the deflection was smaller as the wire tensioning technique was significantly improved. Approximatively 10% of the wires of the prototype could not be tensioned due to broken tensioning pins; only very few pins used with the production modules broke.

7. Shipping and installation of modules onto ZEUS

7.1. Shipping of modules

Completed modules or stacked sections were shipped from ANL to DESY (22 completed modules), from KFA to DESY (10 completed modules), from ANL to KFA (10 EMC sections) and from KFA to ANL (2 HAC sections). To assure secure transportation, the modules were installed in a shipping fixture located inside a 6 m long oceangoing container. Fig. 19 shows a photograph of the shipping fixture containing a module for transportation.

The modules are held by twelve bolts to the stands and the shipping base which in turn is suspended by six pneumatic damping pads mounted on a steel I-beam base frame. Four damping pads are located under the base and two on top of the I-beam frame. The pneumatic system was designed to absorb all shock loads up to 5g acceleration in any direction, even at high frequencies. A compressor system located inside the container and running off 220 V or 110 V, supplies the pneumatic dampers with air during transportation. The frame and module mounting can withstand low-frequency, $5g$ shocks even if the pneumatics are inoperable. Special end brackets were used to support the ends of the EMC sections.

When shipped to DESY the containers were loaded at ANL onto a truck and driven to Montreal (Canada) where they were transferred by sea to Hamburg. At the Hamburg harbour the containers were again loaded onto a truck and driven to the DESY site. The transportation was generally monitored by accelerometers mounted on the shipping frame and on the module itself.

To meet the installation schedule four containers were used. A round trip ANL–DESY–ANL typically took 3–4 weeks.

7.2. Preparation of modules before installation

After unloading from the shipping container at DESY, the modules were visually inspected for any damage which might have occurred during transportation. The modules were then connected to a test station capable of measuring the DU current, carrying out laser light studies and performing scans with ^{60}Co sources. The HV settings required to achieve the nominal DU current in each PMT and the results from the source scans were compared to the corresponding set-

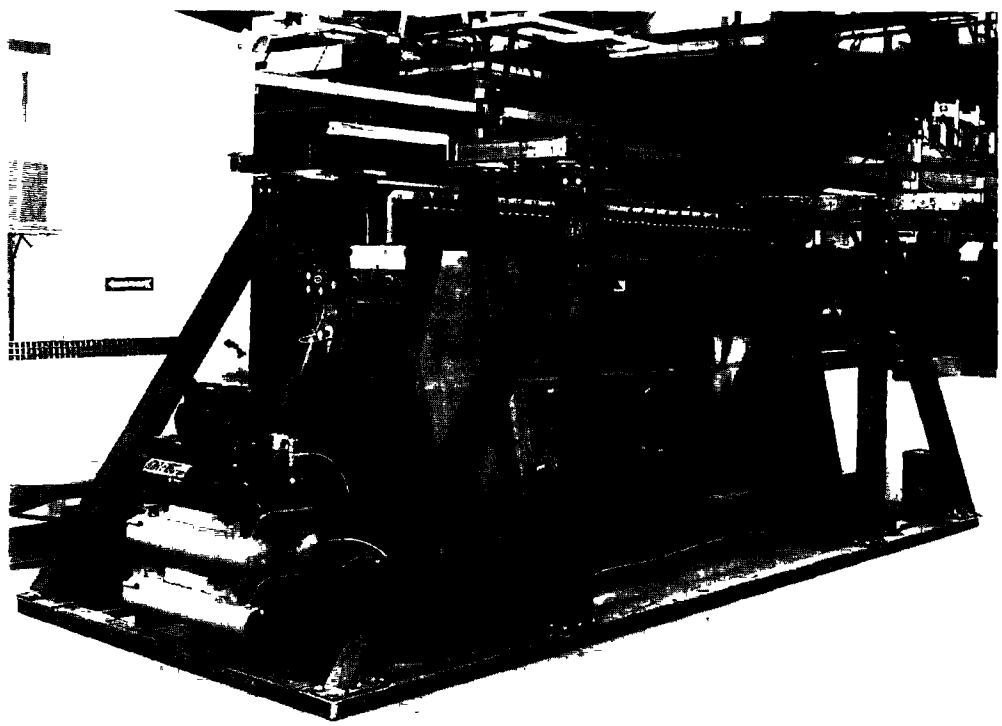

Fig. 19. The shipping fixture containing a module ready for transportation.

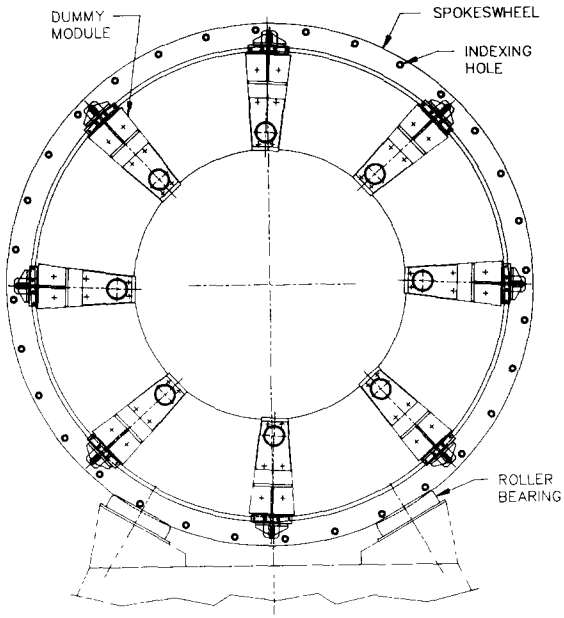

Fig. 20. Spokeswheel arrangement with the dummy modules.

tings and results obtained before transportation. No significant differences were observed for any of the 32 modules.

7.3. Installation procedure

The modules are mounted on ZEUS between the two large aluminum spokeswheels as previously discussed. A nominal 1 cm clearance is allowed at each end to ensure that the modules will fit even in the presence of some distortion of the spokeswheels. During the preassembly of the spectrometer and to provide for mapping of the magnetic field, the spokeswheels were held apart, as shown in fig. 20, by eight dummy modules consisting of a real T-beam and steel end plates, but with the DU-scintillator stack replaced with an aluminum tube. These dummy modules were removed, one by one, as the final modules were loaded into the structure.

The spokeswheel assembly rests on four sets of rollers and can be indexed 1/32 of a revolution at a time using the holes shown in fig. 20. This allows for the insertion of the modules from the top, one by one. To keep a reasonable balanced load, the following loading sequence was used: i) load two modules, rotate 180°; ii) load five modules, rotate 180°; iii) load seven modules, rotate 180°; iv) load eight modules, rotate 180°; v) load seven modules, rotate 180°; vi) load the final three modules. These final three modules are scheduled to be inserted in September 1991 following the beam testing at Fermilab.

The modules' end plates are attached to the spokeswheels by six M20 bolts at each end. The top pair of bolts go through the end plates and into the end of the T-beam, as seen in fig. 4. The nominal 1 cm space between the module and the end plates is closed by brass cylinders that thread into the aluminum spokeswheels using steel helicoils. In addition, at the outer radius, brackets, which are mounted around the

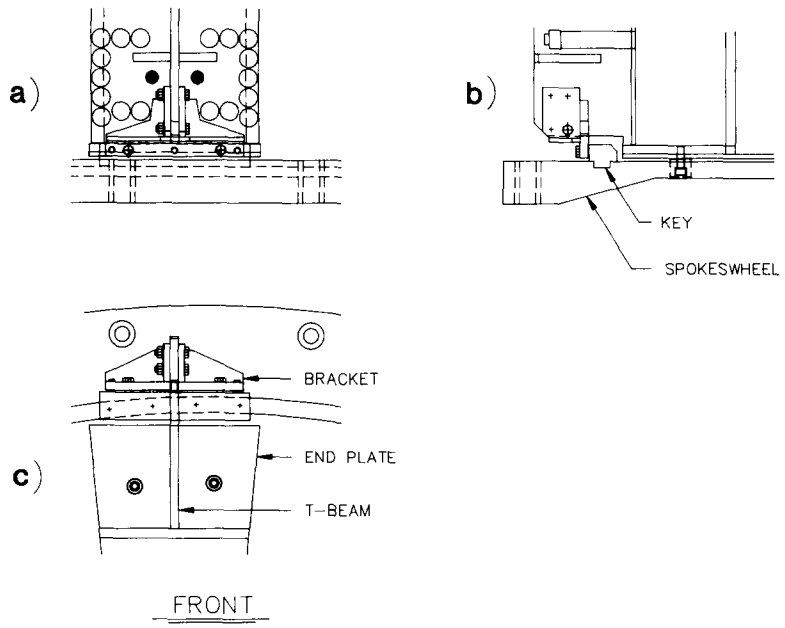

Fig. 21. End bracket arrangement showing the attachment of a module to the spokeswheel: (a) top view; (b) side view; and (c) front view.

T-beam web, attach to keys that are bolted into a machined groove in the spokeswheels, as shown in figs. 4 and 21.

After locating and locking the spokeswheels at the required angle, a module was lowered between them with one module face and the end plates vertical. A special lifting fixture was used on the crane to allow for such an adjustment. When the module was at the appropriate depth, the keys were inserted in the spokeswheel grooves and attached by the four bolts. The module was then lowered further such that part of the weight was taken on the center bolt of the bracket. Adjustment of this bolt set the radial position of the module. A special gauge that pinned into the indexing holes at the outer radius of the spokeswheels was used, together with a rod mounted from the T-beam web at the module center, to check the azimuthal alignment. Feeler gauges were used to ensure that the module-to-module gap at the top end of the end plates was set correctly. The modules were set at the required 1 cm gap from the rear spokeswheels with the front gap allowed to float. The brass inserts were then screwed in to lock the z position of the module.

A rectangular hole at an inner radius of the spokeswheels was used to access the module end plates. Metal blocks were bolted to the module end plate and to the spokeswheels and screws were used to adjust the angle, both at the front and at the rear. The six M20 bolts were then inserted and tightened on each end, the bolts connecting the bracket to the key were tightened, the lifting fixture was removed, and the spokeswheels were indexed to the next position. The full operation took typically one to two hours.

Special attention was given to ensure a proper module-to-module gap in the EMC region, since this is where the modules are structurally the weakest. The design gap is 2 mm. Before insertion, the size of the modules was checked to ensure that they would fit within the allowed envelope.

8. Time scale and personnel

8.1. History of module production

Design work for the prototype modules started in January 1986 and soon after approval of the technical proposal for the ZEUS detector, bids were requested for the production of the prototype HAC mechanical structure. By December 1987 the HAC box had been delivered and the first half of 1988 was dedicated to the construction and study of the steel plate prototype of the HAC and the EMC test section. In the second half of the same year the DU plate prototype module was stacked and early in 1989 the optical system was installed and thoroughly tested.

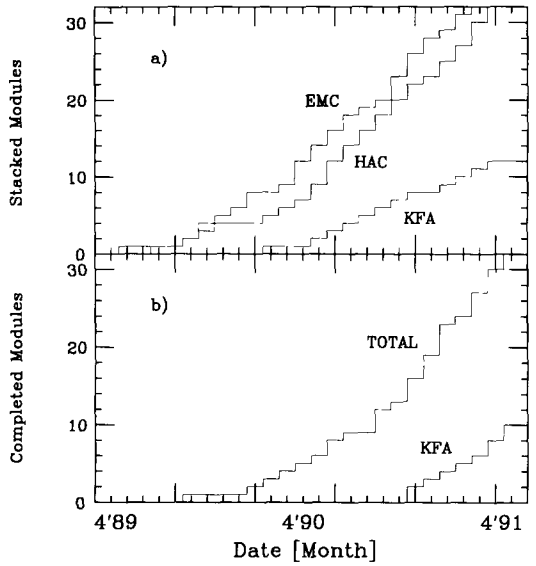

Fig. 22. History of module production: (a) number of stacked sections vs time; (b) number of completed modules vs time.

The construction of the production modules was initiated in April 1989, see fig. 22a. After a slow learning period, modules were stacked at an approximately constant rate of 1.7 modules/month. The pace was generally set by the availability of parts. Fig. 22b shows the number of completed modules vs time. The rate increased from ~ 1 to ~ 2 modules/month with the start of the assembly operations at KFA. All 32 modules were completed by April 1991.

8.2. Manpower

Typically, the construction of one module required 42 man-days for the cladding operation, 30 (8) man-days for stacking the HAC (EMC) section and 20 man-days for mounting the optical readout system and the covers. The four operations proceeded in parallel and to some degree independently of each other. For most of the construction period 12 technicians at ANL and 5 technicians at KFA worked full time on this project.

9. Summary

The design and construction of the barrel calorimeter for the ZEUS detector has been described. The calorimeter consists of depleted uranium plates interleaved with plastic scintillator. The modules of the barrel calorimeter are held together in compression using straps for the HAC and wires for the EMC.

This design minimized the effects of structural components on the energy resolution and homogeneity of the response. The response to electrons and photons

incident close to the intermodule gap is uniform to $\pm 5\%$ owing to the 2.5° tilt of the modules and the addition of 1.6 mm of lead between the modules.

The modules were assembled at ANL and KFA Jülich, Germany. Construction of the entire BCAL spanned two years employing a crew of 17 full time technicians. After a slow turn on period the average production rate reached ~ 2 modules/month.

Acknowledgements

Early development work on the prototype module was done by M. Shackelford (ANL). J. Biggs (ANL) supervised the stacking of this module. The mechanical design was checked by a finite-element analysis done by A. Bühring (ANL).

The following technical support people are heartily acknowledged for their hard work and dedication which made the construction of the ZEUS BCAL possible: A.D. Caird, D.A. Carbaugh, C.W. Keyser, S. Kaminskas, L. Kocenko, D.J. Morgan, J. Pace, R.R. Rezmer, H.V. Rhude, R.J. Rutkowski, K.E. Stair, R.J. Taylor, E.C. Theres, K.L. Wood from ANL and J. Ermel, K. Häusler, R. Janes, R. Schommer, R. Sengstacke from KFA.

Special thanks go to N. Paul (KFA) and T. Romanowski (Ohio State University) who supervised the operations at KFA. J. Nasiatka (ANL) contributed significantly to the shipping of the modules. The installation on ZEUS was supervised by T. Winch (DESY) and D. Reeder (University of Wisconsin).

We also wish to thank our colleagues from Columbia University, Louisiana State University, Ohio State University, Pennsylvania State University, Virginia Polytechnical Institute and State University, and University of Wisconsin for their invaluable intellectual and technical contributions. Last, but not least, we would like to acknowledge the many constructive comments from other members of the collaboration, especially, R. Klanner, B. Löhr, G. Wolf, and W. Zierold (DESY).

This work was supported in part by the U.S. Department of Energy, Division of High Energy Physics, under contract W-31-109-ENG-38.

References

[1] The ZEUS Detector, Technical Proposal of the ZEUS Collaboration, DESY (1986);
The ZEUS Detector, Status Report, DESY PRC 89-01 (1989).

[2] J Brau and T. Gabriel, Nucl. Instr. and Meth. A238 (1985) 489;
H. Brückmann et al., Nucl. Instr. and Meth. A263 (1988) 136;
R. Wigmans, Nucl. Instr. and Meth. A265 (1988) 273.

[3] E. Bernardi et al., ZEUS Note 87-039 (1987);
R. Klanner, Nucl. Instr. and Meth. A265 (1988) 200;
G. d'Agostini et al., Nucl. Instr. and Meth. A274 (1989) 134.

[4] B. Anders et al., Nucl. Instr. and Meth. A277 (1989) 56.

[5] W.R. Nelson, H. Hirayama and D.W.O. Rogers, The EGS4 Code System, SLAC Report 265 (1985).

[6] J. Repond, EGS calculations for the ZEUS barrel calorimeter, AMZEUS Note-61 (1988);
J. Repond, EGS calculations for the ZEUS barrel calorimeter II, AMZEUS Note-66 (1988).

[7] B.G. Bylsma et al., Nucl. Instr. and Meth. A305 (1991) 354.

[8] J. Whitmore et al., AMZEUS Note-105 (1990).

[9] U. Mallik, Proc. 1st Int. Conf. on Calorimetry in High Energy Physics, eds. D.F. Anderson et al. (World Scientific, Singapore, 1991) p. 116

[10] Specifications for the depleted uranium plate contract for the ZEUS barrel calorimeter, AMZEUS Note-72 (1988).

[11] J. Repond, Test of BCAL modules with cosmic rays, AMZEUS Note-106 (1990).

[12] B. Lu et al., The Cockcroft–Walton photomultiplier tube base and the Ethernet high voltage controller, VPI-1 HEP 91/1, submitted to Nucl. Instr. and Meth.

[13] M. Shackelford, ZEUS barrel calorimeter: structural test data, AMZEUS Note-16 (1986);
S. Campione, L. Kocenko and B. Musgrave, Tests of tensioning members for the ZEUS barrel calorimeter, AMZEUS Note-35 (1987).

[14] J. Biggs et al., Stacking and mechanical testing of the prototype BCAL module AMZEUS Note-59 (1988).

[15] A. Bühring, Two dimensional finite element models of a ZEUS barrel calorimeter module box structure, AMZEUS Note-27 (1987);
A. Bühring, Finite element analysis of the ZEUS barrel calorimeter, AMZEUS Note-43 (1987).

[16] Orpheus Harp, M. Derrick et al., AMZEUS Note-54 (1988);
Orpheus Harp II, E. Balabanis et al., AMZEUS Note-67 (1988).